CFD simulation of water diffusion in fruit drying: case of apricot hemispheres

Alkistis Sempou[1], *Diamanto* Lentzou[2], *Athanasios* Athanasiou[2], *Andreas* Boudouvis[1], and *Georgios* Xanthopoulos[2*]

[1]School of Chemical Engineering, Natl. Technical Univ. of Athens, 9 Heroon Polytechniou Str., 15780, Zografou, Greece

[2]Dept. of Natural Resources Management and Agricultural Engineering, Agricultural Univ. of Athens, 75 Iera Odos Str., 118 55, Athens, Greece

Abstract. Food drying is a storage process during which the available water is removed. The present analysis conducted for three drying temperatures 45, 55 and 65 °C and the effective water diffusivity was estimated as 1.69×10^{-10}, 2.91×10^{-10} and 6.67×10^{-10} m^2/s. Comsol Multiphysics 4.3b was used to model the problem and simulate the process. The apricot hemispheres shrinkage was modelled as function of moisture content reduction. The results showed that water diffusivity, the mass transfer coefficient between the fruit surface and drying air and the activation energy of the process increase with drying temperature. The mass transfer coefficient, k_m, was estimated as 1.0×10^{-5}, 9.98×10^{-5} and 0.85×10^{-2} m/s at 45, 55 and 65 °C. The estimated activation energy was 59.6, 59.9 and 60.8 kJ/mol at 45, 55 and 65 °C. The average relative error between experimental and computational moisture content was 0.47, 0.88 and 1.32% at 45, 55 and 65 °C. The Levenberg-Marquardt (L-M) and Sparse Non-Linear Optimizer (SNOPT) optimization algorithms were implemented.

1 Introduction

In a *direct* problem, the diffusion coefficient is incorporated into water diffusion equation in the computer model, which then predicts domain shrinkage and moisture content reduction. However, it is established that the water diffusion coefficient is dependent on both the processing temperature and the moisture content. Therefore, it cannot be considered constant. In order to resolve the *inverse* diffusion problem, it is necessary to determine the diffusion coefficient from supplementary data. The most well-known method for calculating the water diffusivity in *inverse* problems is by the Finite Element Method (FEM). In particular, the problem to be presented introduces the experimental data of the moisture content versus drying time, as well as the volume reduction rate (shrinkage) and determines the water diffusion coefficient, the mass transfer coefficient and the external surface resistance of apricot employing an optimisation procedure.

* Corresponding author: xanthopoulos@aua.gr

2 Theory

During the isothermal drying phase, where fruit of volume V (m^3) and surface A (m^2) reaches the air drying temperature, *Fickian* diffusion is expressed as

$$\partial c/\partial t = \nabla \cdot \left(D_{eff} \nabla c \right), \; 0 \le r < R, \; t > 0 \text{ and } c = c_o, \; t = 0, \text{ in } 0 \le r \le R_o \quad (1)$$

where c is the bulk (locally average over all phases) water concentration in the fruit in mol/m^3 and D_{eff} is its effective water diffusivity (m^2/s). To deal with the complexity of the various drying mass transfer mechanisms (liquid, vapour diffusion, capillary) internal mass transfer mechanisms are incorporated in the D_{eff}. In fruits drying, due to high initial moisture content, it is important to consider shrinkage in the mass transfer analysis. R_o and R are the initial and mean geometric equivalent radius (m) at time t of the drying samples considering the apricot as a hollow sphere. D_{eff} was described by an Arrhenius-type equation,

$$D_{eff} = D_o \exp\left(-E_a / R_u T \right) \quad (2)$$

where E_a is the activation energy (J/mol), R_u is the universal gas constant (J/mol K), D_o is the pre-exponential parameter (m^2/s) and T is the temperature (K). The water content dependence of D_{eff} is satisfied by a modified Arrhenius-type Equation 3.

$$D_{eff} = D_o exp\left(-E_a / R_u T + a/MR \right) \quad (3)$$

where MR is the moisture ratio and D_o=1.0 m^2/s. Saravacos and Maroulis [1] reported values of 10^{-11}-10^{-9} m^2/s for food and fresh products. The D_{eff} values in the literature should be treated with caution, as many are greater than the values reported for water self-diffusion. The water self-diffusion coefficient measured by Nuclear Magnetic Resonance (NMR) has been found as 3.601×10^{-9} m^2/s (45 °C), 4.368×10^{-9} m^2/s (55 °C) and 5.089×10^{-9} m^2/s (65 °C). The mass transport across the air/fruit interface is

$$-\mathbf{n} \cdot (D_{eff} \nabla c) = k_c (c_b - c_i), \quad r = R, \quad t > 0 \quad (4)$$

where **n** is the unit vector normal to the domain boundary (apricot surface), k_c is the mass transfer coefficient (m/s), c_b is the water concentration in the air adjacent to fruit surface (mol/m^3), c_i is the water concentration at the fruit surface (mol/m^3). The inverse of the mass transfer coefficient (r) is the surface resistance to mass transfer and, according to Van der Sman [2] is composed from the resistance of the peel (r_{peel}) and that of the diffusive air film adjacent to the fruit surface (r_{dbl}). For still air, the mass transfer resistance of the air around a sphere is equal to R/D_v [3], where D_v is the diffusivity of water in air and is in the range $6.0\text{-}7.0\times10^2$ s/m (45-65 °C). This range is three orders of magnitude smaller than the r_{peel}, and thus has been assumed that the k_c is due to the peel resistance (r_{peel}), neglecting the resistance due to the diffusive boundary layer (r_{dbl}).

$$r_{total} = r_{peel} + r_{dbl} = r_{peel} \approx k_c^{-1} \quad (5)$$

where r_{peel} is the external surface resistance of apricot (s/m), r_{dbl} is the diffusive boundary layer resistance (s/m) and k_c is the mass transfer coefficient (m/s). The surface resistance

can be analysed by the mass transfer Biot number, $Bi_m=(K\ R/D_{eff})/(1/k_c)$ for a sphere, where K is the surface equilibrium condition (or distribution coefficient) (mol/m^3 in air)/(mol/m^3 in fruit), $c_b=K\ c_i$. The equilibrium water content (kg_w/kg_{dm}) was estimated as 0.47 at 45 °C, 0.33 at 55 °C and 0.32 at 65 °C. Since k_c is defined in relation to the ambient air, K allows Bi_m to be related to the resistance between the surface and the air. In a *direct* problem with the boundary condition (BC) (Equation 4) and the initial condition (Equation 1), the mass transfer properties $D_{eff}=f(T, MR)$ and k_c are all specified and then the problem given by Equations (1,3,4) is concerned with the determination of the water content distribution in the fruit as a function of time and position.

In the *inverse* problem, $D_{eff}=f(T,MR)$ (Equation 3) and the mass transfer coefficient k_c (Equation 4) are unknown and are estimated by solving *Fick's* law of diffusion (Equation 1) employing the experimental drying curves, $M_{wb}=f(t)$ over the drying period. For this reason, the *L-M* optimisation algorithm and the FEM were combined to estimate $D_{eff}=f(T, MR)$ and k_c in an *inverse* mass transfer problem taking place during convective drying of apricots with shrinkage. The shrinkage was measured experimentally and taken into account in the overall solution. The optimisation was based on minimising the distance between the simulation and the experimental drying curves, $M_{wb}=f(t)$. The *L–M* algorithm was chosen due to its superior convergence rate associated with the *Least-Squares*-type problems such as the one at hand. The *L-M* algorithm combines two minimisation algorithms, the *Gradient Descent* or *Steepest Descent* and the *Gauss-Newton*. The former is suitable for large numbers of optimisation parameters, while the latter, is suitable for medium-sized problems and converges faster. The transition between the two algorithms is controlled by a *damping factor* [4].

3 Computational model

The physical problem under consideration gives rise to a computational model for deriving theoretical predictions of the spatio-temporal distribution of water content in drying halved apricots as a function of D_{eff}, peel resistance and shrinkage. The governing equations along with the boundary and initial conditions were numerically discretised by the FEM using Comsol Multiphysics 4.3b [5]. The mesh was structured and consisted of ≈2,765 elements and ≈228 boundary elements (Figure 1).

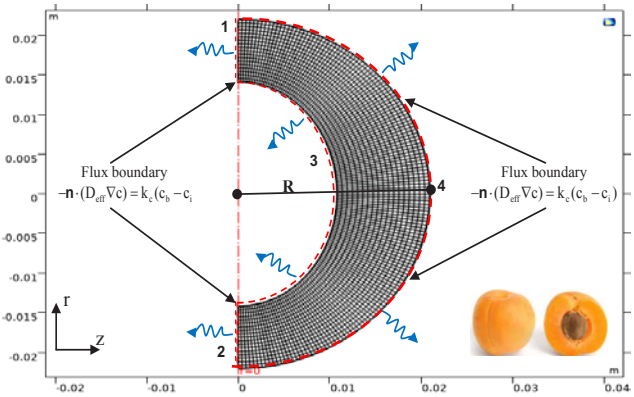

Fig. 1. Geometry, discretisation of the shrinking domain and flux boundary conditions (1-4). The embedded photo corresponds to whole and half apricot sample.

This time-dependent problem was solved by an implicit time-stepping method known as the *Backward Differentiation Formula*. The resulting system of nonlinear PDEs in the time-space domain was solved numerically by coupling the FEM with the Arbitrary *Lagrange–Eulerian* (ALE) method to account for the domain shrinkage. In the ALE method, the boundary conditions control the displacement of the moving mesh with respect to the initial geometry. The displacement of the moving boundary is propagated throughout the domain to obtain a mesh deformation using the *Laplace* smoothing technique. The volume change due to shrinkage was assumed to be equal to the amount of water removed (ideal shrinkage). The resulting non-linear system of equations was solved using *Newton's* method. At each iteration step, the linearized system was solved using the *Parallel Sparse Direct Solver*. The time step was set to one hour although Comsol Multiphysics 4.3b implements an internal variable time step to meet the relative (0.0001) and absolute tolerance (0.00001) [4]. The optimisation problem was run on a PC with quad-core processors (64-bit 3.60GHz per core) and 12 GB of RAM. The reliability of the solutions was verified by grid independence tests.

4 Materials and methods

4.1 Drying experiments arrangement

The experiments were carried out with apricot hemispheres (var. *Tom Cot*). The drying took place in a Binder FD115 oven (BINDER Gmbh, Germany). The initial water content was 8.01±1.3 kg_w/kg_{dm} (45 °C), 7.99±1.2 kg_w/kg_{dm} (55 °C) and 7.20±0.8 kg_w/kg_{dm} (65 °C). The air temperature and humidity were monitored by Hobo 8H sensors (Onset Computer Corp., Southern MA, 146 USA) and measurements were logged in a HOBO Micro Station Data Logger H21-002 (Onset Computer Corp., Southern MA, USA). The samples were weighed using an FY-300 with an accuracy of ± 0.02g and a resolution of 0. 01g. The samples dimensions were measured by a thickness gauge of ±0.02 mm precision and the volume was estimated by the immersion method. Three drying temperatures were tested 65 °C, 55 °C and 45 °C. Fourteen apricot hemispheres with no stone were used per drying temperature. Ten samples were used for weight measurement per hour and four for volume estimation every two hours. Drying was ended when the dimensionless moisture content was MR_f=0.1. The drying lasted 13h at 65 °C, 22h at 55 °C and 40h at 45 °C. Upon completion of drying, the dry matter per sample was determined at 105 °C for 24h.

4.2 Evaluation of volume and shrinkage velocity

The mean volume of the drying samples was estimated based on the geometric mean $\bar{V} = \sqrt[n]{\prod_{i=1}^{n} V_i}$, V_i, the experimental volume. The initial volume ranged between 10.79 cm^3 and 15.99 cm^3 while apricot stone thickness ranged 10.54-13.08 mm. In all the drying cases, the shrinkage ranged between 82-85% of the initial volume. To integrate the ALE into the mathematical model, the shrinkage velocity was estimated for the MR range 1.0 - 0.1. Based on the statistical analysis (Statgraphics Centurion XVI, Statpoint Technologies Inc, VA, USA) the shrinkage velocity was expressed as the ratio of apricot radius reduction per drying time as a function of the MR, R/t=f(MR) (Figure 1). From this analysis, Equations (6a-c) derived and adopted in the computational model.

$$45\ ^{o}C,\ R/t=exp(-16.97+4.75\times MR),\qquad R^2_{adj}=99.25 \quad (6a)$$
$$55\ ^{o}C,\ R/t=exp(-16.30+4.28\times MR),\qquad R^2_{adj}=99.58 \quad (6b)$$

65 °C, $R/t=exp(-15.86+4.08\times MR)$, $R^2_{adj}=99.14$ (6c)

The apricot external radii, R were estimated from the mean experimental apricot volume per drying case, based on Equation 7,

$$R=\sqrt[3]{\frac{3}{2\pi}\bar{V}+R^3_{stone}} \quad (7)$$

4.3 Computational implementation

For the development of the computational model, the *Fickian* water diffusion model (Equation 1) was applied in a moving mesh combined with an optimisation model to estimate the k_c, E_a and a. The D_{eff} was taken by a modified *Arrhenius*-type Equation 3. The problem was posed and solved in a hemispherical domain employing the BCs (labelled as 1-4 in Figure 1), of the mass flux type (Equation 4). The concentration of water in the samples is given by

$$c_i=M_{wb}\rho_{prod}/M_w \quad (8)$$

where M_{wb} is the water content on wet basis (kg_w/kg_{prod}), ρ_{prod} is the density of the fruit (kg_{prod}/m^3_{prod}) and M_w is the water molecular weight (0.018 kg_w/mol). The following assumptions were adopted: -initial water concentration was uniformly distributed and experimentally estimated; -drying samples were homogeneous hemispheres with volume equal to the true volume; -D_{eff} was assumed to be isotropic and temperature and water dependent, varying in time and space; -mass transfer through the apricot mesocarp was by diffusion only; -deformation was equal to water volume loss; -water evaporation took place at the air/fruit interface. In our study, the *L-M* with 2 nd order numerical gradient approximation was chosen as the optimisation algorithm in order to achieve improved computational accuracy.

Inverse problems do not have a unique solution, making their solution prone to error if only the minimisation of the objective function is considered. Therefore more criteria were implemented for the choice of the final optimisation parameters such as (i) $D_{eff}=10^{-11}$-10^{-9} m^2/s where most of the food D_{eff} have been reported [1]; (ii) difference between the estimated and experimental final volume less than 5%; (iii) predicted D_{eff} less than water self-diffusion; (iv) estimated and experimental water content difference per case less than 3%.

5 Results and discussion

The computational model was simplified considering a homogeneous isotropic mesocarp under apricots' peel. The initial considered values for the k_c was 0.001 m/s, for E_a; 55,000, 59,000 and 65,000 J/mol for 45, 55 and 65 °C and for *a*, 0.10. In all the cases, the predicted and experimental moisture contents differed less than 1.5% (Table 1).

In Figure 2, the predicted radius R reduced by 50% at 45 °C and 55 °C, based on Equation 7, indicated that the computational model predicted an 80% reduction of samples volume, result that is in agreement with the experimentally estimated shrinkage which ranged between 82-85%. While at 45 and 55 °C the radius decreased from 0.022 to 0.011m (50% radius reduction, i.e. 80% volume reduction), at 65 °C the final radius was 0.013 m, 2

mm higher than the other two cases. This is due to the fact that as the drying temperature increases, shrinkage becomes more intense and drying deviates from ideal drying.

Table 1. Estimated k_c, E_a, a, for the apricot hemispheres, with the MRE (%), mean D_{eff} and surface resistance r_{peel} values.

Temperature (°C)	RH (%)	k_c (m/s)	r_{peel} (s/m)	E_a (kJ/mol)	a	MRE (%)	$\bar{D}_{eff} \times 10^{-10}$ (m^2/s)
45	15	1.00×10^{-5}	1.00×10^{5}	59.6	0.104	0.47	1.69
55	10	9.99×10^{-5}	1.00×10^{4}	60.0	0.009	0.88	2.91
65	6	0.85×10^{-2}	1.18×10^{2}	60.8	0.052	1.32	6.56

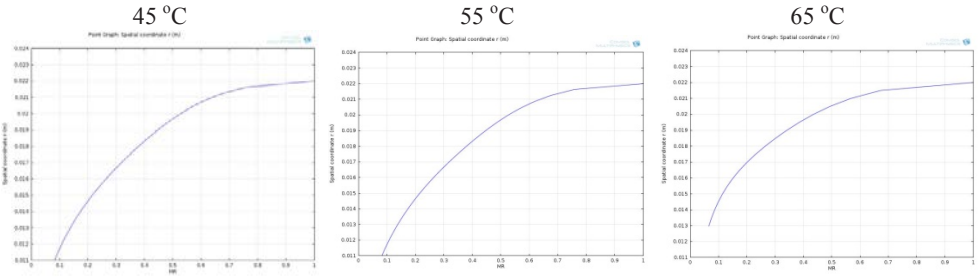

Fig. 2. Shrinkage in terms of R reduction, as function of MR for the three drying temperatures.

In Figure 3 is presented the experimental and simulated moisture content of apricot hemispheres at three drying temperatures in which can be seen that is in good agreement.

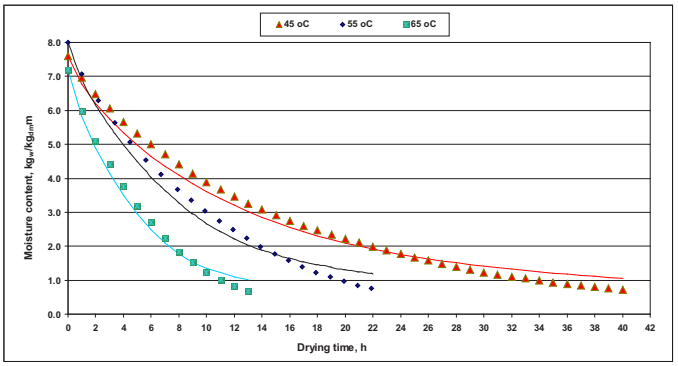

Fig. 3. Experimental (points) vs predicted (lines) moisture content from the proposed program regarding the three drying temperatures.

The estimated E_a lie within the range reported for dried agricultural products [4]. The comparison should be carried out with great caution, taking into account different drying methods (convective, microwave or combined), mathematical analysis (analytical: *method of slopes, regular regime method* or numerical solution of water transport equations) and applied BCs (*Dirichlet*, *Neumann* type), as well as varieties with different physiology and anatomy (peel, m esocarp, endocarp). O therwise, t he drawn co nclusions co uld b e misleading. The E_a ranged from 59-61 kJ/mol for apricot hemispheres (Table 1). From the

tabulated values (Table 1), can be concluded that the criteria for self-diffusion of water [D_{eff}: 3.6×10^{-9} m^2/s (at 45 °C), 4.37×10^{-9} m^2/s (at 55 °C) and 5.09×10^{-9} m^2/s (at 65 °C)] are satisfied along with the values of the D_{eff} which is ranged between 10^{-11}-10^{-9} m^2/s. Shrinkage is a significant component of drying modelling as it affects D_{eff} due to the shortening of water diffusion paths as can be seen in the 3-D imaging of Comsol output (Figure 4).

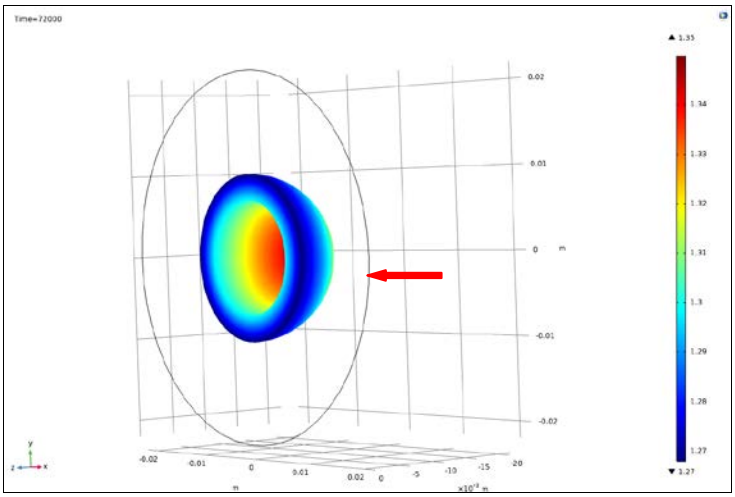

Fig. 4. 3-D imaging of MC_{dm} (kg_w/kg_{dm}) and shrinkage of the apricot hemisphere at 55 °C and time of 20 h. The line (red arrow) is the initial (t=0 h) circumference of apricot's hemisphere.

In all the tested cases, the D_{eff} increases in the initial drying phase (Figure 5), but to a different degree, due to the product temperature increase and, to a lesser extent, to the water content reduction. From this observation, it can be concluded, that the steep increase in D_{eff} in the initial drying stages, is not only temperature driven, but also depends on the water transport rate from the inner product to the surface of the drying product. The latter is affected by the physical structure of the peel, which varies among fruits and to the best of our knowledge, has not been taken into account in any water transport model. Such information is very crucial for drying optimisation since highlights the significance that flesh and skin have into drying process and in overall in the energy needed to conduct the drying process.

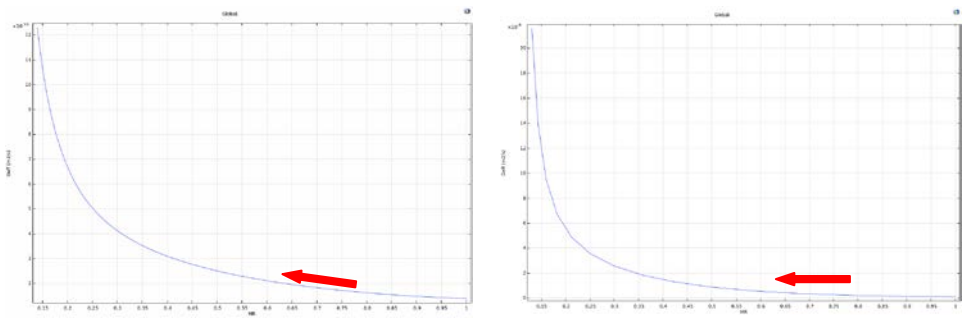

Fig. 5. The predicted D_{eff} as a function of MR reduction (red arrow) at 45 °C (left) and 65 °C (right).

The optimised E_a and a and the resulting mean geometric D_{eff} are shown in Table 1. The effect of the drying temperature in D_{eff} is depicted in Figure 6 as well in Table 1. The estimated k_c and that of the peel resistance $r_{peel}=1/k_c$ are tabulated in Table 1. The r_{peel} (Table 1) exhibits a decreasing order as the drying temperature increases but further study is needed since the predicted r_{peel} includes the area of peel (exocarp) as well the flesh (endocarp) in dried apricot hemispheres. As has been discussed, information regarding the water transport in the flesh and peel of the apricot is important for drying optimisation. Since this process is energy-consuming, is crucial to identify the way these two anatomical features change, in which extent, and under which conditions. This information can improve not only the energy efficiency of the drying but also the quality of the final product.

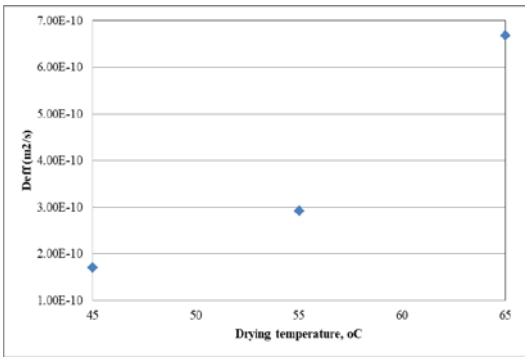

Fig. 6. The mean D_{eff} of apricot hemispheres for the three drying temperatures.

Values of r_{peel} for drying apricot hemispheres cannot be found in the literature, so the comparison of results was based on Pham [6] experiments. Although these results are not directly comparable since they involve different products, whole apples [6] and in our study apricot hemispheres, the order of magnitude of k_c is in the range of 5×10^{-7} - 20×10^{-7} m/s [6], while in this study it is in the range of 10^{-7} - 10^{-2} m/s.

6 Conclusions

In this study the macroscopic sources of modelling limitations derived from fruit's complex and inhomogeneous anatomy have been identified. The D_{eff} of apricot hemispheres was estimated and found to range between 1.69×10^{-10} - 6.56×10^{-10} m^2/s. The r_{peel} of apricot hemispheres was found to be 1.18×10^{2} - 1.0×10^{5} s/m. Further study is needed experimentally and computational to evaluate the values of D_{eff} and r_{peel} for the area of peel as well for the flesh in the dried apricot hemispheres.

References

1. G.D. Saravacos and Z.B. Maroulis, Transport properties of foods, (Marcel Decker, New York, 2001).
2. R.G.M. Van der Sman, Simple model for estimating heat and mass transfer in regular-shaped foods. J Food Eng. **60**, 383-390 (2003). https://doi.org/10.1016/S0260-8774(03)00061-X

3. R.B. Bird, W.E. Stewart and E.N. Lightfoot, Transport phenomena, (John Wiley & Sons, New York, 2002).
4. D. Lentzou, A.G. Boudouvis, V.T. Karathanos, G. Xanthopoulos, A moving boundary model for fruit isothermal drying and shrinkage: An optimization method for water diffusivity and peel resistance estimation. J Food Eng, **263**, 299-310 (2019). https://doi.org/10.1016/j.jfoodeng.2019.07.010
5. COMSOL Multiphysics, Chemical engineering module model library, (COMSOL AB, Stockholm, 2007).
6. Q.T. Pham, W. Schotsmans, Q.T. Ho, B.E. Verlinden, P. Verboven, B.M. Nicolaï, Simultaneous measurement of neon diffusivity and skin resistance of 'Braeburn' and 'Jonica' apples, Postharvest Biol Tec, 50(1), 53-63 (2008). https://doi.org/10.1016/j.postharvbio.2008.04.002